Granular Matter (2018) 20:81
https://doi.org/10.1007/s10035-018-0853-7

ORIGINAL PAPER

Sand–rubber mixtures undergoing isotropic loading: derivation and experimental probing of a physical model

Auriane Platzer[1,2] · Salman Rouhanifar[3] · Patrick Richard[1] · Bogdan Cazacliu[1] · Erdin Ibraim[3]

Received: 27 March 2018 / Published online: 3 November 2018

Abstract
The volume of scrap tyres, an undesired urban waste, is increasing rapidly in every country. Mixing sand and rubber particles as a lightweight backfill is one of the possible alternatives to avoid stockpiling them in the environment. This paper presents a minimal model aiming to shed light on the relevant physical parameters governing the evolution of the void ratio of sand–rubber mixtures undergoing an isotropic compression loading, where the mixtures consist of various volume ratios of rubber. It is based on the idea that, when pressure is applied, the rubber particles deform and partially fill the porous space of the system, leading to a decrease of the void ratio with increasing pressure. We show that our simple approach is capable of reproducing experimental data obtained with sand and rubber of similar particle size distributions up to mixtures composed of 50% of rubber. The effect of the particle shape and size on the model parameters is discussed.

Keywords Sand · Rubber particle · Mixture · Isotropic loading · Experiment · Modelling

1 Introduction

The number of scrap tyres is increasing rapidly in both developed and developing countries due to the steady rise in the number of vehicles. Consequently, the accumulation of used tyres is gradually becoming a real societal problem. In this context, recycling and mixing rubber particles derivatives with granular soil particles constitute a solution to this problem as they can be used in various geotechnical applications such as backfilling for retaining structures, slope and highway embankment stabilization, road constructions, soil erosion prevention and seismic isolation of foundations [1]. In addition to their remarkable mechanical properties [2–7], such soil-rubber chip composite mixtures have interesting acoustical and drainage properties too [8].

While their potential range of applications is wide, a full understanding of their behaviour, including internal interaction mechanisms resulting from the combination of two particular materials, one soft, tyre chip rubber, and one rigid, granular soil, requires further studies despite recent interesting works [9–13]. Existing studies reveal complex behaviours whose mechanisms are difficult to understand and which originate from the heterogeneity of such mixtures as a consequence of the high stiffness contrast of constituents. The complexity of the behaviour of the composite also results from the characteristic geometrical contrasts of the particles, either the aspect ratio (particle length to breadth) of the soft particle, or the rubber to sand particle size ratio [10,14–16]. As for any geotechnical system, the practical use of these mixtures requires the development of numerical analyses which are normally based on adequate constitutive models. A classical way to reach this goal is to use homogenization approaches based on the so-called rule-of-mixture [17–23] . Yet such approaches, which assume no correlation between the behaviours of the two constituents, are not well adapted to predicting the mixture behaviour resulting from the high stiffness contrast of constituents [24] like sand–rubber mixtures. The high deformation of rubber particles inevitably influences the positions of sand grains and thus the global response of the sample to an applied stress. For the same reasons classical Discrete Element Methods (DEM) [8,10,11,25] in which

✉ Erdin Ibraim
erdin.ibraim@bristol.ac.uk

1 IFSTTAR, MAST, GPEM, 44340 Bouguenais, France

2 GeM (Institut de recherche en génie civil et mécanique), CNRS UMR 6183, École Centrale de Nantes, 44321 Nantes, France

3 Department of Civil Engineering, University of Bristol, Bristol, BS8 1TR, UK

grains are modeled by spheres are restricted to very small strains since they do not take into account the change in shape of rubber particles, as consequence of their deformation. These types of simulations are thus not able to reproduce the influence of the shape modification mentioned above on the geometrical properties of the material. Although continuum constitutive models describing the behaviour of such mixtures are scarce, one can note a hypoplastic model based on the critical state framework developed in [2]. Note also that, alternative modelling approaches (e.g. the Material Point Method [26] or a recent DEM-based modelling [27] that, unlike classical DEM, take into account grains' deformability) are promising. Consequently, in a near future, we can expect to see more realistic grain-scale simulations of such sand–rubber particulate composites.

Here, we present a simple model based on assumed soft-rigid interactions at particle scale aiming to point out some of the main physical insights of the aforementioned behaviour. We focus our study on the evolution of the void ratio as observed in experiments on small scale samples made of coarse and fine grains under isotropic compression loading. Various volume ratios of rubber are considered, but to reduce the parameter space we only focus on mixtures composed of rubber and sand particles of similar particle size distributions. It should be pointed out that our approach adopted here is phenomenological with the aim to shed light on the main mechanism governing the void ratio decrease of a mixture undergoing an isotropic compression. The present work is a first stage towards our long term objective which is the development of a continuum constitutive model whose parameters retain a physical meaning and which applies to a wide range of cases where the sand particles and the rubber particles significantly differ in size.

The outline of our paper is the following. First, we present our physical model, its assumptions and its predictions. Section 3 is devoted to the presentation of materials, laboratory set up and experimental results. Then, the application of the model to those experiments is presented for a granular mixture composed of coarse and rounded particles (Sect. 4). In Sect. 5, we probe and discuss the physical hypothesis by comparing the results of our model predictions with experimental results obtained for mixtures of finer and sub-angular sand grains. Finally we present our conclusions.

2 Model

To derive our model we consider a granular packing made of sand grains and rubber particles. The volume ratio of rubber, x_R, is defined as the ratio $V_R/(V_R + V_S)$ where V_R and V_S are respectively the solid volumes of the rubber and sand. For the sake of simplicity, we focus here on packings for which all the sand or rubber particles have the same size distribution. By this, we ensure that the grading of the sand–rubber mixture does not evolve and remains independent of the volume ratio of rubber. We also limit the development of the model to the behaviour under isotropic compression loading of the materials for which we analyze the evolution with the pressure of the void ratio i.e. the ratio between the volume of the porous space and the volume of the solids. The isotropic behaviour of sand samples, $x_R = 0$, is considered to be known and is an input of our model which is designed to predict the volumetric changes under isotropic stresses of granular sands with non-rigid rubber inclusions, $x_R > 0$.

2.1 Preliminary assumptions

Our model is based on the following preliminary assumptions:

1. Sand grains are infinitely rigid, and the volumetric changes in the pure sand sample ($x_R = 0$) are a consequence of particle re-arrangements;
2. Rubber chip particles are incompressible (material Poisson's ratio approximately 0.5, consequently V_R is also constant);
3. The repartition of rubber particles is spatially homogeneous within the mixture;
4. The studied sand–rubber mixtures are isotropic and remain isotropic under an isotropic loading;
5. While the sand–rubber system under isotropic compression undergoes volumetric changes, these are a consequence of both particle re-arrangement and rubber particles' deformability;
6. Finally, we restrict ourselves to pressures important enough to probe the properties of the granular material, not those of the grain surface. Consistently with the literature, we choose $p > p^* \approx 100$ kPa.

The threshold pressure mentioned in the last preliminary assumption can be estimated by considering two spherical sand grains of equal size (diameter D) interacting through the Hertz' law. To achieve a deformation of the order of magnitude of the surface's asperities ($\delta \approx 100$ nm), it is necessary to apply a macroscopic pressure $p^* = \kappa\delta^{3/2}/D^{3/2}$, κ being a constant which depends on Young's modulus E and on Poisson's ratio ν through $\kappa = 4E/\left[3\pi(1-\nu^2)\right]$. Using $E = 90$ GPa, $\nu = 0.4$ leads to $p^* \approx 100$ kPa for D of a few tenths of millimeter. This threshold pressure represents an upper limit for sand–rubber mixtures considering that the other types of contact provide a much lower pressure. Note that, due to the two first preliminary assumptions, the volume ratio of rubber, x_R, is constant whatever the loading conditions.

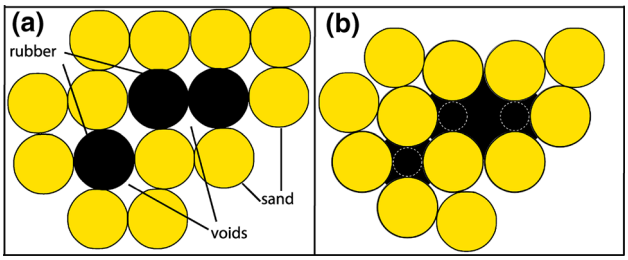

Fig. 1 Sketch explaining the mechanism of void filling by the deforming particles: we assume that, due to the deformation of rubber particles, the porous space of (**a**) an initially undeformed packing is (**b**) partially filled by the rubber

2.2 Volumetric evolution

The volumetric evolution of the sand–rubber granular packing is determined by the following two-step rule.

1. Firstly, the volumetric changes due to the sand–rubber particle re-arrangement equal those of the sand sample, $x_R = 0$, at equal isotropic pressures. We remind here that the size distribution of the two solid phases is the same irrespectively of the volume ratio of rubber x_R.
2. Subsequently, under isotropic loading, a fraction of the porous space is filled by the deforming rubber particles. It is further considered that the rubber particles are virtually divided into two zones: one that participates to the loading transmission alongside granular side particles and one that is not transferring any loading thus acting like a void inert portion (see Fig. 1).

Compared to the volume of the porous space of the granular soil ($x_R = 0$), the volume of the porous space V_V of a sand rubber mixture, x_R, at a given isotropic pressure, p, can be written in the following form:

$$V_V(x_R, p) = V_V(x_R = 0, p) - f(x_R, p) x_R (V_S + V_R), \quad (1)$$

where the function f is the deformed fraction of rubber and is given by the total volume of rubber that fills the porous space once the rubber particles deform to the total volume of rubber. The deformed fraction of rubber depends on both the volume ratio of rubber x_R and on the isotropic pressure p. In the following we will derive an expression relating f to these two quantities. Note also that we only consider mixtures which have identical initial void ratios whichever the volume the rubber ratio, i.e initial means fabrication at an unloaded state (Fig. 2). For a given x_R, the evolution of deformed fraction of rubber, f, with the pressure is intuitive: at the early stages of the isotropic compression process, the available pores are large and easy to fill. Consequently, f increases with the pressure. As the pores get filled, it becomes more and more difficult to fill the remaining porous space and

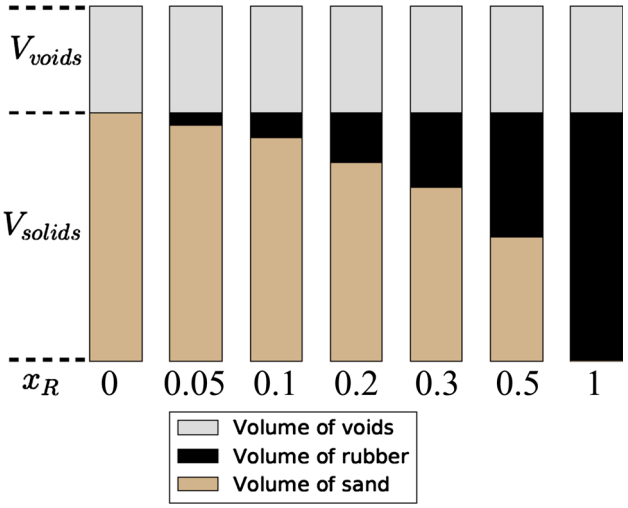

Fig. 2 Sketch of the composition of the sand–rubber mixtures studied. The void ratio is constant whatever the rubber ratio

f reaches a constant value. The final assumption we make is thus the following: the simplest way to model such an increase towards a saturation value is to assume that f obeys the following first order differential equation:

$$p_0(x_R) \left.\frac{\partial f}{\partial p}\right|_{x_R} + f(x_R, p) = F(x_R), \quad (2)$$

where $p_0(x_R)$ is a characteristic pressure and $F(x_R)$ the maximum deformed fraction of rubber for an infinite pressure, i.e $f(x_R, p \to \infty)$. Such an equation is classically used to model systems involving both a driving force and viscous-like force. For example the fall of an object in a viscous fluid (the system is driven by gravity and slowed down by viscosity) and the loading of a capacitor (the system is driven by an electromotive force and slowed down by the Ohm law) are described by similar equations. Here, the system is driven by the compression pressure and slowed down by the ability of the porous space to resist to the rubber filling (i.e. a permeability-like quantity). Intuitively, for a given volume ratio of rubber, x_R, both p_0 and F are function of the geometry of the porous space: small pore sizes lead to significant values of p_0 compared with media with high pore sizes, whereas the maximum deformed fraction of rubber, F, should increase with the minimum void ratio of the pure sand packing which in turn may depend on particle shape. These two quantities will also depend on the rubber volume ratio, x_R, and for a given pressure variation and similar porous size, obviously less porous volume will be filled by the deformed rubber of a mixture with low volume rubber ratio in contrast with a mixture with high volume rubber ratio. Thus, a decrease of p_0 and an increase of F with x_R are intuitively expected. Young's modulus of the rubber particles also has an obvious effect on the characteristic pressure since it would

require a larger pressure to deform stiffer rubber particles. From a dimensional analysis we expect a proportional relation between this Young's modulus and p_0. The solution of Eq. (2) is given by:

$$f(x_R, p) = f^* + \left(F(x_R) - f^*\right)\left[1 - \exp\left(-\frac{p - p^*}{p_0(x_R)}\right)\right], \tag{3}$$

where $f^* = f(x_R, p = p^*)$. The parameters $p_0(x_R)$ and $F(x_R)$, discussed above, are unknown functions of x_R that can be easily determined from experiments. Indeed, $\log \partial(f - f^*)/\partial(p - p^*)$ is an affine function of the adjusted pressure $p - p^*$ whose intercept and slope are respectively given by $\log\left[\left(F(x_R) - f^*\right)/p_0(x_R)\right]$ and $-1/p_0(x_R)$.

Although it is probably possible to have a direct estimation of $f(x_R, p)$ quantity using X-ray tomography at several stages of the compression process, in the absence of such experimental results we test our model by studying the evolution of the mixture void ratio with the mean pressure in small scale sample isotropic compression tests. The void ratio $e_p(x_R, p) = V_V/(V_S + V_R) = e(x_R = 0, p) - x_R f$ predicted by our model can be obtained by combining Eqs. (1) and (3) :

$$e_p(x_R, p) = e(x_R = 0, p) - f^* x_R - x_R\left(F(x_R) - f^*\right)\left[1 - \exp\left(-\frac{p - p^*}{p_0(x_R)}\right)\right], \tag{4}$$

where $e(x_R = 0, p)$ is the experimental void ratio obtained at a pressure p for a pure sand material and $f^* = \left(e_p(x_R, p^*) - e(x_R = 0, p^*)\right)/x_R$. This prediction requires the knowledge of (i) the evolution of the void ratio versus the pressure for a pure sand sample ($x_R = 0$), (ii) the parameter p_0 (the characteristic pressure) and (iii) the parameter F (the maximal deformed fraction of rubber). These three prerequisites a priori depend on the type of sand, rubber and their physical characteristics (e.g contact friction, sand and rubber stiffness) used but the importance of this dependence on the behaviour of the mixture is an open question that will be discussed in the next sections. However, in any case, the effect of rubber stiffness, the granular packing of the sand, the friction between rubber–rubber, rubber–sand and sand–sand contacts are implicitly embedded in these two model parameters F and p_0. An explicit formulation between the grains characteristics and the model parameters requires a different modelling approach which is out of the scope of this paper. For the sake of clarity, in the remainder of the paper, we will use e and e_p for the experimental void ratio and the void ratio predicted by our model respectively. Note that in Eq. (4) the void ratio of the pure sand sample appears explicitly. Thus our theory can be seen as a perturbation of this sample induced by the presence of rubber particles. Consequently it is only valid for sand–rubber composites and not for full sand or rubber materials. We will test our model up to a rubber fraction equal to 0.5.

3 Experiments

We will compare the findings and predictions of our model with laboratory experimental results. For this study, we have chosen two silica based uniform sand materials, Leighton Buzzard (LB) fraction A characterised as a coarse material (mean grain diameter, $D_{50} = 1.6$ mm, coefficient of uniformity, $C_u = D_{60}/D_{10} = 1.3$, coefficient of gradation, $C_g = D_{30}^2/(D_{60}D_{10}) = 1.02$) and Hostun RF (HS) characterised as fine material (mean grain diameter, $D_{50} = 0.38$ mm, coefficient of uniformity, $C_u = 1.7$, coefficient of gradation, $C_g = 1.1$). These materials are well known and widely used in laboratory testing e.g. [28–31]). The rubber particles are obtained from the shredding of used lorry tires and consist of polymer, acetone, carbon black, ash and Sulphur. Following a tedious process that involved washing, drying, sorting and sieving, equivalent rubber granular materials have been engineered to match the particle size distributions of both sands. A selection of typical rubber chip particles that mirror both the LB and the HS sands are shown in Fig. 3a, b,

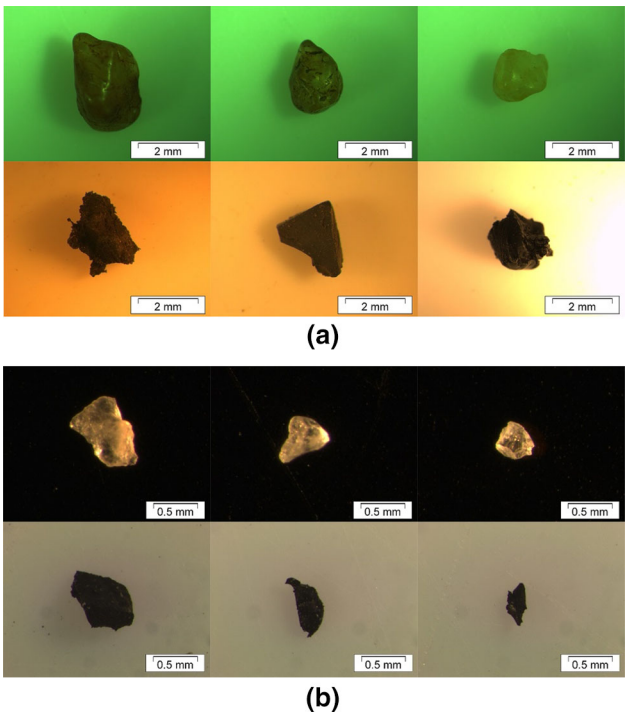

Fig. 3 Individual particles of sand (top) and equivalent rubber chip particles (bottom) for **a** the Leighton Buzzard sand and **b** the Hostun RF sand

Table 1 Void ratios of the samples after application of a small vacuum of 20 kPa at various rubber volume fractions x_R

Leighton Buzzard sand–rubber mixtures $e_{min} = 0.55$, $e_{max} = 0.83$		Hostun RF sand–rubber mixtures $e_{min} = 0.62$, $e_{max} = 1.00$	
x_R	Void ratio	x_R	Void ratio
0.	0.630	0.	0.746
0.05	0.627	0.05	0.741
0.1	0.625	0.1	0.739
0.2	0.620	0.2	0.736
0.3	0.618	0.3	0.736
0.5	0.604	0.5	0.719
1.	0.602	1.	0.707

e_{min} and e_{max} are minimum and maximum void ratios respectively

respectively. The fabrication process of all samples of cylindrical shape (70 mm diameter and 70 mm height) is done using the moist tamping technique [32]. The method implies the succession of three stages: mixing of constituents, deposition and compaction [2,33–35]. Sand and rubber particles are mixed by adding 10% water content and the mixture is placed into the triaxial cylindrical mould in three successive layers. Each layer is compacted up to a pre-definite height using a circular tamper with a diameter half the size of the sample diameter. While this technique appears to be more effective in discouraging segregation of the composite constituents, providing good control of sample density and homogeneous distribution of rubber, it also produces a soil-rubber fabric which may correspond to that obtained in rolled-compacted construction fills. Once the sample is fabricated, a top cap together with a lateral latex membrane seal the sample and a small vacuum of approximately 20 kPa is applied. This vacuum is necessary for the protection of the sample's fabric and stability during removal of the cylindrical mould.

Note that, the initial void ratios of sand alone samples have been chosen to have the same initial relative density $D_r = (e_{max} - e)/(e_{max} - e_{min}) = 66\%$ where e, e_{max} and e_{min} are respectively the in situ void ratio, the maximum void ratio corresponding to a very loose state and the minimum void ratio corresponding to a very dense state. Considering the technical limitations associated with the laboratory determination of the minimum and maximum void ratios of the sand–rubber composites, for a given sand and sand–rubber mixture type and for comparison purposes, an identical fabrication target void ratio was fixed for all samples. Although the fabrication target void ratio was set identical for all the samples, at this stage, due to the compressible nature of the rubber and membrane flexibility, a slight variation of the void ratio for various volume ratios of rubber, $x_R = 0.0,\ 0.05,\ 0.1,\ 0.2,\ 0.3,\ 0.5$ and 1.0, was recorded as reported in Table 1.

The triaxial cell containing the cylindrical sample is then filled with water and pressurized to a pressure of 30 kPa while the vacuum is released. All samples are saturated by applying CO_2 for around 45 min followed by flushing de-aired water to obtain a Skempton coefficient (B) higher than 95%. A back-pressure of 100 kPa is normally used. Both the back pressure and cell (total pressure) pressure are measured by pressure transducers. The samples are then loaded isotropically up to a maximum pressure of 550 kPa. During the isotropic compression, the sample volumetric changes are measured by a volume change measurement device accounting for the amount of water that is expelled in the process.

The experimental evolutions of the void ratio e versus the pressure p for Leighton Buzzard sand–rubber are reported as an example in Fig. 4a. As expected the void ratio decreases with increasing pressure and the higher the volume ratio of rubber, the stronger the decrease. The use of the rule-of-mixture, based on the void ratio weighted mean approach, is not able to capture the evolution of the curve $e(p)$ with the volume ratio of rubber, because this method does not take into account the interactions between phases and the individual contributions of each component to the overall mixture response are scaled according to their fraction. We have reported its predictions for $x_R = 0.3$ in Fig. 4a as well as the error between the prediction of the rule-of-mixture and the experimental results for all volumetric rubber fractions in Fig. 4b. The error remains systematically significant for all the values of the pressure p and the volume ratio of rubber used with a maximum error close to 6%. The calibration of p_0 and F model parameters is first made for LB sand–rubber mixtures in the next section. The validation follows and is done based on HS sand–rubber mixture experimental results.

4 Calibration of the physical model

In this section, we will apply our model to the case of Leighton Buzzard sand–rubber mixtures. The calibration process provides the empirical evolution of both the characteristic pressure p_0 and the maximum deformed fraction of rubber F with x_R for this type of sand. Both quantities are

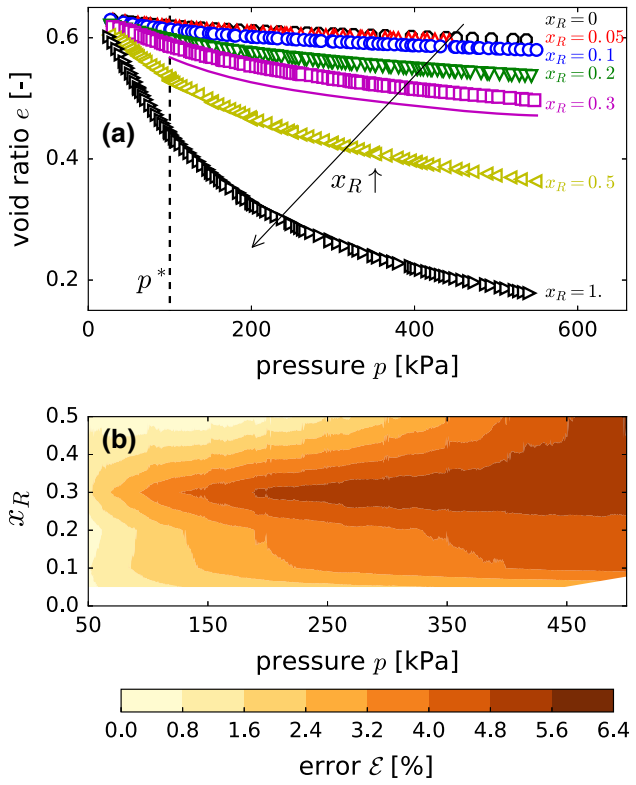

Fig. 4 **a** An isotropic compression of sand–rubber mixtures made with Leighton Buzzard sand leads to a decrease of the void ratio e with pressure. We have used $x_R = 0., 0.05, 0.1, 0.2, 0.3, 0.5$ and 1.0 (the increase of x_R is indicated by the arrowed line). The solid line represents the prediction of the rule-of-mixture for $x_R = 0.3$ and the vertical dashed line corresponds to $p = p*$ the pressure above which the properties of the granular material are probed, not those of the grain surface (see 6th preliminary assumption in Sect. 2.1). **b** The error $\mathcal{E}$ between the prediction of the rule-of-mixture and the experimental results is weak ($< 6.5\%$) but systematic for any values of the pressure and of the volume ratio of rubber

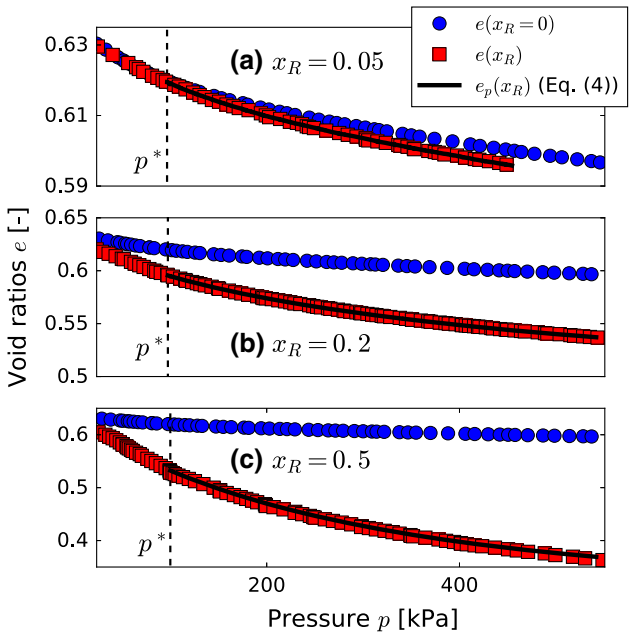

Fig. 5 Comparison between experimental void ratios and those obtained by our model for several volume ratios of rubber and the Leighton Buzzard sand for **a** $x_R = 0.05$, **b** $x_R = 0.2$ and **c** $x_R = 0.5$. Squares (resp. circles) correspond to the sample with rubber ($e(x_R, p)$) (resp. without rubber $e(x_R = 0, p)$) and the solid line to the prediction of our model $e_p(x_R, p)$. As in Fig. 4, the vertical dashed line corresponds to $p = p^*$

obtained by fitting $\log \partial(f - f^*)/\partial(p - p^*)$ by an affine function (see Sect. 2).

We have reported in Fig. 5 the evolution of the void ratio versus the applied pressure for materials obtained for $x_R = 0.05$ (Fig. 5a), $x_R = 0.2$ (Fig. 5b), and $x_R = 0.5$ (Fig. 5c). We also include in those subfigures the curve obtained for $x_R = 0$ as well as the fit of the experimental data by our model [Eq. (4)]. The good fit between the model and the experimental data (Fig. 5) indicates the suitability of Eq. (4) to describe the proposed internal deformation mechanism of the sand–rubber mixture under isotropic compression loading. Figure 6 reports the variations of the fit parameters F and p_0. As expected, the maximum deformed fraction of rubber, F, increases with x_R and, in the considered range, this increase is reasonably captured by the linear variation $F(x_R) = F_{model}(x_R) \approx 0.1 + 0.95\, x_R$. The characteristic pressure p_0 is found to decrease with x_R. Yet, this decrease is so small that, for the sake of simplicity, we assume that $p_{0,model}$ is a constant equal to 296.6 kPa. Of course, since the comparisons between the experimental and theoretical void ratios have been made using the empirical expression of p_0 and F, the observed good agreement is not surprising (error inferior to 1%). We just show that the theoretical prediction of the deformed fraction of rubber f is not incompatible with experimental results. To probe more deeply our model we have to discuss its potential application to the other type of sand we have used: the Hostun RF sand.

5 Experimental probing of physical insights

To validate our approach, we use the expressions of p_0 and F obtained in Sect. 4 for Leighton Buzzard sand—rubber mixtures, i.e. F_{model} and $p_{0,model}$, for the Hostun RF sand–rubber mixtures. For that purpose we carried out isotropic compression tests of sand–rubber mixtures. We determine the theoretical evolution of the void ratio e with the applied pressure p by means of Eq. (4) in which we use $F_{model} = 0.1 + 0.95\, x_R$ and $p_{0,model} = 296.6$ kPa as well as the evolution of the void ratio with the pressure in the case of a pure Hostun RF sand material. Figure 7 reports experimental curves as well as the corresponding prediction of our model.

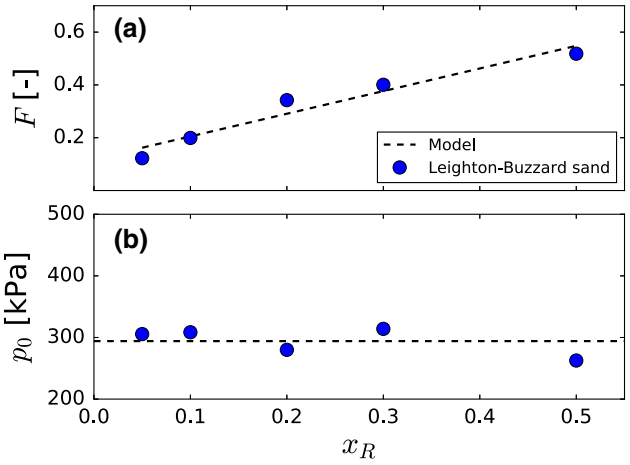

Fig. 6 **a** The evolution of F, the maximum deformed fraction of rubber, is affine with x_R in the studied range of x_R ($F = 0.1 + 0.95\,x_R$). **b** In contrast, the pressure p_0 characterizing the exponential decay of the void ratio versus the applied pressure is almost constant with the volume ratio of rubber ($p_0 \approx 296.6$ kPa)

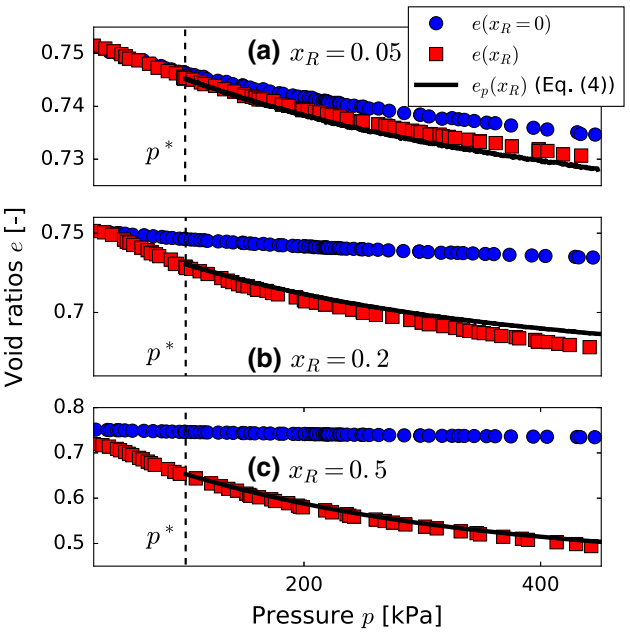

Fig. 7 Comparison between experimental void ratios and those obtained by our model for several volume ratios of rubber and the Hostun RF sand for **a** $x_R = 0.05$, **b** $x_R = 0.2$ and **c** $x_R = 0.5$. Squares (resp. circles) correspond to the sample with rubber ($e(x_R, p)$) (resp. without rubber $e(x_R = 0, p)$ and the solid line to the prediction of our model $e_p(x_R, p)$. As in Fig. 5, the vertical dashed line corresponds to $p = p^*$

The correspondence is fairly good, highlighting the quality of our approach. Yet such a good correspondence may be surprising. Indeed, the parameters F and p_0, which are respectively the maximum deformed fraction of rubber and the characteristic pressure of the filling of the pores by the rubber, should depend on the porous space geometry and thus on the shape of grains. Yet, the Leighton Buzzard sand is rounded whereas the Hostun RF sand is sub-angular and, consequently, the geometry of the porous space different. To explain this apparent contradiction, two limiting cases should be considered: (i) the case where x_R is small and (ii) the case where x_R is large. In the former, the difference between $e(x_R = 0)$ and $e(x_R)$, i.e. $x_R\, f$, is small enough so that the effect of the grains' shape on the values of p_0 and F is almost negligible on $e(x_R)$. In other words, if x_R is small, $x_R\, f \ll e(x_R) - e(x_R = 0)$ whatever the type of sand used. In the latter case, the behaviour of the mixture is mainly controlled by the rubber (see below), so the effect of the grains' shape becomes negligible. To confirm this point, we have reported in Fig. 8 the error between the predictions of our model and the experimental results as a function of pressure and rubber ratio. It shows that the error is maximum for high pressures and $x_R = 0.3$. Interestingly, this value corresponds to a rubber volume ratio, $x_R \approx 0.3$, below which the behaviour of the mixture is mainly governed by that of the sand packing (i.e. its behaviour is sand-like) and, in contrast, above which the behaviour is governed by the rubber packing (i.e. its behaviour is rubber-like) as frequently reported in various experimental studies in the literature [10,14,15,36,37]. As mentioned in Sect. 2.1 in our model, the volumetric changes of the sand–rubber composites originate from (i) the rearrangement of the sand particles and (ii) the deformability of the rubber particles. Thus $x_R \approx 0.3$ seems to correspond to the rubber fraction for which the sum of these two contributions is the least estimated by our model: the volumetric changes assigned to sand rearrangement are not perfectly captured due to relatively large rubber fractions and the rubber particles' deformation is underestimated, probably as a consequence of structure effects that are not taken into account by our model. It is also worth noting that the error map is not symmetric with respect to the $x_R = 0.3$ axis showing the different importances of the volumetric changes assigned to sand rearrangement prevailing for $x_R < 0.3$ and of those assigned to rubber deformability prevailing for $x_R > 0.3$.

In this section, we have compared the prediction of our model to experimental results obtained on Hostun RF sand. For this, we used $p_{0,model} = 296.6$ kPa and $F_{model} = 0.1{+}0.95\,x_R$, expressions obtained with another type of sand: the Leighthon Buzzard sand. To go further in the probing of our model we can compare the values of the two aforementioned parameters to those obtained by fitting directly the results obtained with the Hostun RF sand (Fig. 9). The characteristic pressure, p_0, obtained by fitting the experimental curves obtained on Hostun RF sand–rubber mixtures decreases with the rubber fraction, x_R, and is greater than that of Leighton Buzzard sand–rubber mixture up to $x_R \approx 0.3$. Above 0.3 volumetric rubber fractions, p_0 becomes independent of the type of sand used, which is consistent with

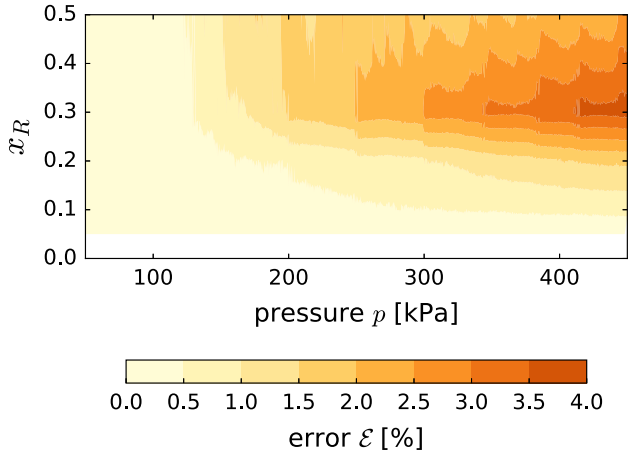

Fig. 8 The error between the prediction of our model and the experimental results for Hostun RF sand–rubber is maximum for a rubber ratio approximatively equal to 0.3 and important pressures ($p \approx 450$ kPa)

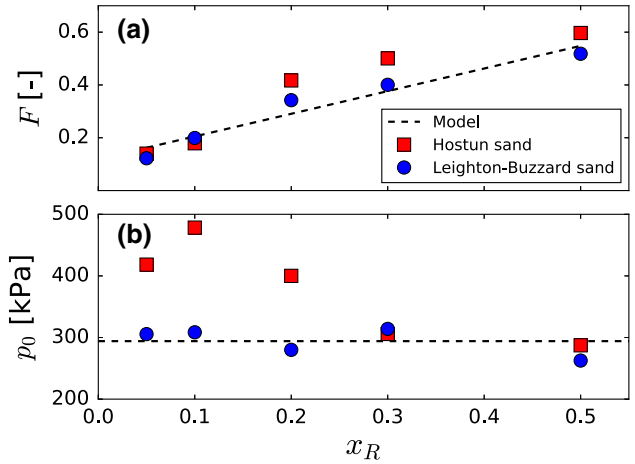

Fig. 9 **a** The maximum deformed fraction of rubber, F, depends weakly on the type of sand (Leighton Buzzard or Hostun RF) and F_{model} captures correctly the experimental values obtained with Hostun RF sand. **b** The characteristic pressure depends on the type of grains for $x_R < 0.3$. Above this value, the behaviour of the mixture is rubber-like, and p_0 becomes independent of the rubber volume fraction

the threshold rubber ratio mentioned above which separates a sand-behaviour from a rubber-behaviour. For rubber fractions greater than 20%, F is slightly larger for Hostun RF sand compared to Leighton Buzzard sand suggesting a possible dependence of F on the grains' characteristics and/or on the minimum void ratio of the sand alone materials. Even so, the trend still can be well captured by the linear expression obtained by fitting the evolution of F versus x_R in the case of Leighthon Buzzard sand. In other words, whatever the properties of the porous space, the maximum deformed fraction of rubber is the same. However, the way in which f increases towards this maximum remains dependent on the porous space through the characteristic pressure p_0. Note that, although at small values of x_R the fitted values of p_0 are significantly larger than $p_{0,model}$ the predictions of the model remain fairly good. Surprisingly, the most important discrepancy between the experimental data and our model is obtained for $x_R = 0.3$, for which the value of p_0 is very close to $p_{0,model}$. Yet, the same rubber ratio corresponds to the biggest difference, although small, between F_{model} and F obtained by fitting the experimental curves. Among the assumptions made, some are fully justified. For example the assumption that sand is incompressible is justified by the value of the Young's modulus of the sand which is three order of magnitude greater than that of rubber. Similarly, assuming the incompressibility of rubber is justified by its Poisson's coefficient whose value is close to 0.5. Other assumptions probably deserve more thorough justifications. Firstly, the range of pressure studied. We indeed assume that our model is only valid for pressures greater than a threshold p^* below which the deformation is too weak to neglect the importance of the surface properties of the grains. As mentioned above, this is common in the field of geotechnics. Relaxing this assumption would require to model the surface properties of both the Hostun RF sand and the Leighton Buzzard sand and include them in the model, which is beyond the scope of this paper. Secondly, we have assumed that the amount of particle re-arrangement is identical at identical pressures for both sand alone and sand–rubber mixtures. Although reasonable in the case of the packings submitted to compression, this is probably no longer the case when the packings are submitted to shear. Thirdly, we have assumed that the rubber grains are homogeneously distributed within the sample. In other words, every rubber grain has, statistically, the same neighbourhood. Clusters are allowed but the probability of existence has to be independent of their position.

Finally, it is worth mentioning two further developments to this work. First refers to adapting our model for packings where sand and rubber particles have different size distributions. Second, as mentioned above, a direct measurement of the deformed fraction of rubber f would be an ultimate test for our model.

6 Conclusions

We derived a simple model aiming to predicting the evolution of the void ratio of granular materials made of mixture of sand grains and rubber particles undergoing isotropic compression. We restricted ourselves to mixtures for which the size distributions of the sand and rubber particles are similar to avoid, at this stage of the work, an evolution of the mixture grading curve with the rubber fraction. Our model assumes that the deformed fraction of rubber, which increases with the pressure, fills the porous space and that its evolution with the pressure obeys a first order equation whose parameters (a characteristic pressure, p_0 and the maximum deformed

fraction of rubber F, both function of the volume fraction of rubber) can be measured from experiments. The characteristic pressure, p_0, is associated to the difficulty for the rubber particles to deform and fill the porous space. Rubber that is more rigid, a granular structure with smaller pore sizes, sand particles of higher angularity or high grain-grain friction coefficients lead to higher values of p_0. The maximum deformed fraction of rubber, F, may depend on the grain characteristics and minimum void ratio of the sand alone material. Interestingly, the nature of the sand (i.e. size and shape) seems however to have a limited effect on those parameters. Although very simple, our model still captures experimental results in a very satisfactory way. Thus our model is able to predict the effect of including soft particles in a material made of rigid grains. It can be applied to any system composed of two types of grains with an important rigidity contrast. However, the model describes an alteration of the behaviour of packing of rigid particles, and is conceived for packings with a majority of rigid particles. Finally, the quality of the model predictions suggests that the particle re-arrangement in sand–rubber mixtures under isotropic loading remains relatively low and close to the particle rearrangement experienced by the sand alone. This may not be the case for generalized loading conditions which may imply significant particle rearrangements and possible additional model parameters are required.

The next step of this study is two-fold. First, we will adapt our model to the cases where the sand particles and the rubber particles significantly differ in size. In such a case, the isotropic behaviour of the pure sand sample with a size distribution equal to that of the sand–rubber mixture will be required. Second, we will evaluate the effect of including rubber particles on the shear mechanical properties of the materials through the development of a continuum constitutive model directly based on the development presented in this paper.

Acknowledgements This work was possible with the financial support of the University of Bristol through the International Strategic Fund programme. Erdin Ibraim initiated this work during a Visiting Professorship (IFSTTAR Nantes) supported by La Région Des Pays de la Loire, France.

Compliance with ethical standards

Conflict of interest There is no conflict of interest.

References

1. Lee, J.H., Salgado, R., Bernal, A., Lovell, C.W.: Shredded tires and rubber–sand as lightweight backfill. J. Geotech. Geoenviron. Eng. **125**(2), 132–141 (1999)
2. Youwai, S., Bergado, D.T.: Strength and deformation characteristics of shredded rubber tire–sand mixtures. Can. Geotech. J. **40**(2), 254–264 (2003)
3. Kaneda, K., Hazarika, H., Yamazaki, H.: Numerical simulations of earth pressure reduction using tire chips in sand backfill. J. Appl. Mech. **10**, 467–476 (2007)
4. Garga, V.K., O'Shaughnessy, V.: Tire-reinforced earthfill. Part 1: construction of a test fill, performance, and retaining wall design. Can. Geotech. J. **37**(1), 75–96 (2000)
5. Poh, P.S.H., Broms, B.B.: Slope stabilization using old rubber tires and geotextiles. J. Perform. Constr. Facil. **9**(1), 76–79 (1995)
6. Bosscher, P.J., Edil, T.B., Kuraoka, S.: Design of highway embankments using tire chips. J. Geotech. Geoenviron. Eng. **123**(4), 295–304 (1997)
7. Tsang, H.-H., Lo, S.H., Xu, X., Neaz Sheikh, M.: Seismic isolation for low-to-medium-rise buildings using granulated rubbersoil mixtures: numerical study. Earthq. Eng. Struct. Dyn. **41**(14), 2009–2024 (2012)
8. Valdes, J.R., Evans, T.M.: Sand-rubber mixtures: experiments and numerical simulations. Can. Geotech. J. **45**(4), 588–595 (2008)
9. Eidgahee, D.R., Hosseininia, E.S.: Mechanical behavior modeling of sand–rubber chips mixtures using discrete element method (DEM). AIP Conf. Proc. **1542**(1), 269–272 (2013)
10. Lee, C., Shin, H., Lee, J.-S.: Behavior of sandrubber particle mixtures: experimental observations and numerical simulations. Int. J. Numer. Anal. Methods Geomech. **38**(16), 1651–1663 (2014)
11. Lopera Perez, J.C., Kwok, C.Y., Senetakis, K.: Effect of rubber size on the behaviour of sand–rubber mixtures: a numerical investigation. Comput. Geotech. **80**, 199–214 (2016)
12. Lopera Perez, J.C., Kwok, C.Y., Senetakis, K.: Micromechanical analyses of the effect of rubber size and content on sand–rubber mixtures at the critical state. Geotext. Geomembr. **45**(2), 81–97 (2017)
13. Lopera Perez, J.C., Kwok, C.Y., Senetakis, K.: Investigation of the micro-mechanics of sandrubber mixtures at very small strains. Geosynth. Int. **24**(1), 30–44 (2017)
14. Zornberg, J.G., Cabral, A.R., Viratjandr, C.: Behaviour of tire shred–sand mixtures. Can. Geotech. J. **41**(2), 227–241 (2004)
15. Kim, H.-K., Santamarina, J.C.: Sand–rubber mixtures (large rubber chips). Can. Geotech. J. **45**(10), 1457–1466 (2008)
16. Lee, C., Hung Truong, Q., Lee, J.-S.: Cementation and bond degradation of rubber–sand mixtures. Can. Geotech. J. **47**(7), 763–774 (2010)
17. Voigt, W.: Ueber die beziehung zwischen den beiden elasticittsconstanten isotroper krper. Annalen der Physik **274**(12), 573–587 (1889)
18. Reuss, A.: Berechnung der fliegrenze von mischkristallen auf grund der plastizittsbedingung fr einkristalle. ZAMM J. Appl. Math. Mech. **9**(1), 49–58 (1929)
19. Villard, P., Jouve, P., Riou, Y.: Modélisation du comportement mécanique du texsol. Bulletin de Liaison Laboratoire Central des Ponts et Chausses **168**, 15–27 (1990)
20. di Prisco, C., Nova, R.: A constitutive model for soil reinforced by continuous threads. Geotext. Geomembr. **12**(2), 161–178 (1993)
21. Ibraim, E., Diambra, A., Muir Wood, D., Russell, A.R.: Static liquefaction of fibre reinforced sand under monotonic loading. Geotext. Geomembr. **28**(4), 374–385 (2010)
22. Diambra, A., Ibraim, E., Muir Wood, D., Russell, A.R.: Fibre reinforced sands: experiments and modelling. Geotext. Geomembr.

28(3), 238 – 250 (2010) (IS Kyushu 2007 Special Issue on New Horizons in Earth Reinforcement)
23. Diambra, A., Ibraim, E., Russel, A.R., Muir Wood, D.: Modelling the undrained response of fibre reinforced sands. Soils Found. **51**(4), 625–636 (2011)
24. Pindera, M.-J., Khatam, H., Drago, A.S., Bansal, Y.: Micromechanics of spatially uniform heterogeneous media: a critical review and emerging approaches. Compos. B Eng. **40**(5), 349–378 (2009)
25. Evans, T.M., Valdes, J.R.: The microstructure of particulate mixtures in one-dimensional compression: numerical studies. Granul. Matter **13**(5), 657–669 (2011)
26. Nezamabadi, S., Nguyen, T.H., Delenne, J.-Y., Radjai, F.: Modeling soft granular materials. Granul. Matter **19**(1), 8 (2017)
27. Asadi, M., Mahboubi, A., Thoeni, K.: Discrete modeling of sand–tire mixture considering grain-scale deformability. Granul. Matter **20**(2), 18 (2018)
28. Naughton, P.J., O'Kelly, B.C.: The anisotropy of leighton buzzard sand under general stress conditions. In: Proceedings 3rd International Symposium on Deformation Characteristics of Geomaterials (IS Lyon03), 2003 22th–24th September, pp. 285 – 291, Lyon
29. Lanzano, G., Visone, C., Bilotta, E., Santucci de Magistris, F.: Experimental assessment of the stress–strain behaviour of leight on buzzard sand for the calibration of a constitutive model. Geotech. Geol. Eng. **34**(4), 991–1012 (2016)
30. Flavigny, E., Desrue, J., Palayer, B.: Note technique : le sable d'Hostun. Revue Française Géotechnique **53**, 67–70 (1990)
31. Doanh, T., Ibraim, E.: Minimum undrained strength of hostun RF sand. Géotechnique **50**(4), 377–392 (2000)
32. Ladd, R.: Preparing test specimens using undercompaction. Geotech. Test. J. **1**, 16–23 (1978)
33. Rao, G.V., Dutta, R.K.: Compressibility and strength behaviour of sand–tyre chip mixtures. Geotech. Geol. Eng. **24**(3), 711–724 (2006)
34. Hazarika, H., Otani, J., Kikuchi, Y.: Evaluation of tyre products as ground improving geomaterials. Proc. Inst. Civ. Eng. Ground Improv. **165**(4), 267–282 (2012)
35. Rouhanifar, S., Ibraim, E.: Mechanics of Soft–Rigid Soil Mixtures, pp. 3329–3334. ICE Publishing, London (2015)
36. Lee, J.-S., Dodds, J., Santamarina, J.C.: Behavior of rigid–soft particle mixtures. J. Mater. Civ. Eng. **19**(2), 179–184 (2007)
37. Rouhanifar,S.: Mechanics of Soft–Rigid Soil Mixtures. Ph.D. thesis, University of Bristol (2017)